Article:

Benvidi, A., Dehcheshmeh, E.M., Safari, P. et al. (2 more authors) (2023) Post-fire seismic performance of low-yielding-steel plate shear wall systems. International Journal of Civil Engineering, 21 (10). pp. 1661-1678. ISSN 1735-0522

https://doi.org/10.1007/s40999-023-00856-y

Post-fire seismic performance of low-yielding steel plate shear walls system

Ali Benvidi[a], Esmaeil Mohammadi Dehcheshmeh[a], Pouria Safari[a], Vahid Broujerdian[a*], Shan-Shan Huang[b]

[a] School of Civil Engineering, Iran University of Science and Technology, Tehran, Iran

[b] Department of Civil and Structural Engineering, The University of Sheffield, Sheffield, UK

Abstract

In this study, the post-fire seismic behaviour of steel structures with a special low-yielding steel plate shear wall system was investigated. Three steel structures of 3, 6, and 9-storey with special moment-resisting steel frames and special low-yielding SPSW were designed according to AISC-360/16, AISC-341/16, and ASCE-07/16 using software CSI ETABS. One 2D frame of each structure was then modelled using the finite element package Abaqus and analysed with the push-over method to determine their response modification factors R, an indicator of the nonlinear seismic performance of a structure. The models were validated against experimental testing on a steel plate shear wall system, which showed good agreement. The post-fire mechanical properties of steel were then implemented into the model and the post-fire response modification factors were determined. According to the results, the post-fire response modification factors of the 3, 6, and 9-storey models could respectively be reduced by 14.9%, 15.9%, and 9.0% compared to those before the fire, showing a considerable reduction in the nonlinear seismic performance of the structures. Furthermore, the results showed that higher temperature with more stories exposed to fire followed by air cooling leads to more reduction in seismic capacity, and overall water cooling tends to reduce the seismic capacity less than air cooling. Also, it was indicated that the code-specified value of R is rather over-conservative for post-fire calculations.

Keywords: Steel Plate Shear Wall, Post-Fire Seismic Performance, Push-Over Analysis, Finite Element Method, Response Modification Factor

1. Introduction

It is probable that fire-induced incidents in steel structures trigger extreme structural damages and even total collapse by imposing large deformations [1]. Even if the fire-induced damages to the

* Corresponding author: Vahid Broujerdian
Postal address: School of Civil Engineering, Iran University of Science & Technology, P.O. Box 16765-163, Narmak, Tehran, Iran. Tel.: +98 21 77240399. Fax: +98 2177240398. E-mail address: broujerdian@iust.ac.ir

structure in case of deformations are not visibly clear, the post-fire rehabilitation can , in many cases, cost much more than applying preventive measures at the design and construction stages of the structure . But, the combination of fire with other hazards, such as earthquake after or before the fire, has drawn much attention amongst researchers because this particular type of multi-hazard can cause even more devastating damages to structures [2] .

Despite the considerable investigation of the shear wall system's behaviour under lateral loads and during (or shortly after) fires, there is a clear need for a better understanding of the response under the combined action of these hazards [3]. Accurate assessment of the performance of steel plate shear wall system after exposure to fire is of paramount importance for several reasons. Even in the best case scenario by observation, if fire becomes suppressed without imposing much damage to the structure , an engineer still needs to assess the residual capacity of the system to decide about repair or replacement . For a relatively mild fire, replacement of the compartment lining material may suffice to rehabilitate the structure, but the possible reduction in capacity due to the thermal exposure nevertheless needs to be quantified. Finally, a reduction in seismic capacity due to fire may imperil a structure's stability during post-fire earthquake response, e.g., in a situation where an earthquake triggers a fire, which in turn is followed by aftershocks [3].

The steel plate shear wall (SPSW) system with its remarkable application in the seismic design of structures is widely being used as a complementary structural system in the structural design of buildings as shown in Figure 1. The concept of the shear walls system dates to the 1930s when the diagonal constant tensile field notion was used for calculating the capacity of a set of panels with rigid flanges and slender webs, which proved that the buckling of the web cannot be considered an indicator of ultimate capacity of the structural system [4].

Compared to other structural systems, the performance of SPSW system in fire condition aside from the type of steel used (hot-rolled or cold-formed) has been studied less than other systems. There seems to be a huge gap in understanding their behaviour when exposed to fire. Recent studies have studied the effectiveness of stiffeners on steel plate shear buckling at ambient and elevated temperatures indicating that the stiffener's role is more of a lateral restraint than a load path for shear forces [5]. Research on the fire performance of cold-formed steel shear wall with different steel grades and thicknesses showed that increasing the stud thickness and the use of high-strength steel results in an increase in the fire-resisting rating [6]. Fire resistance of cold-formed steel-framed shear walls under various fire scenarios was experimentally tested and it highlighted differences in the thermal response and subsequent performance of the walls as well as different sensitivity of the walls to pre-damage condition during an earthquake [7]. Examination of the structural response of cold-formed steel-framed systems under combinations of the simulated earthquake and fire loading showed a progressive decrease of post-fire lateral load capacity with increasing fire intensity [8]. Numerical modelling of the post-fire performance of strap-braced cold-formed steel shear walls suggested that the post-fire lateral capacity of the walls can be predicted from ambient temperature methods with the use of the cold-formed steel residual mechanical properties [9]. Post-earthquake fire testing of a mid-rise cold-formed steel-framed building was carried out experimentally and seismic design parameters were inferred from the measured structural response [10 and 11]. The performance of SPSW under fire condition was examined and it was revealed that heat exposure negatively affects the seismic performance of SPSW by reducing 95% of its lateral strength under sustained high temperatures [12]. The influence of fire on the seismic shear capacity of cold-formed steel shear walls was experimentally investigated in a set of tests, and initial tests on earthquake-damaged steel sheathed cold-formed steel shear walls under fire load showed a change in failure mode from local to global buckling and highlighted the significance of the response of the gypsum board on the overall fire and load-bearing behaviour [13]. Finite element analysis of the lateral capacity of cold-formed steel shear walls after fire exposure indicated that the lateral behaviour of the walls depends primarily on the imposed maximum temperature on the cold-formed steel members, and the resulting residual material properties [14]. The behaviour of steel-sheathed shear walls subjected to seismic and fire loads was assessed experimentally and the test results indicated that the fire exposure caused a shift in the failure mode of the walls from local buckling of the steel sheet in cases without fire exposure to global buckling of the steel sheet with 35% reduction in lateral load capacity after the wall was exposed to fire [3].

In addition, regarding the post-fire behaviour of steel, a comprehensive research review did an extensive literature survey and by analysing the effects of fire on mechanical properties of the steel, it showed that cold-formed steel can be more affected by fire exposure than hot-rolled type [15]. Investigating post-fire mechanical properties of steel with various cooling methods showed that predictive stress-strain models based on experimental tests can be useful tools for fire safety research studies [16-19]. More importantly, it was shown that rapid water cooling has a great negative impact on the cyclic behaviour of steel which can seriously compromise the seismic performance of steel structures in a post-fire earthquake scenario [20-22].

Also, the influence of fire scenario on the seismic performance of steel structures equipped with steel plate shear walls in post or pre-fire cases is quite unclear because various factors such as fire load density, the location where fire starts, and the direction which fire spreads can affect the performance such systems [23 and 24], and until now, there has not been any research study on this specific subject.

Still, more research should be carried out on this subject to fully understand the mechanisms of failure, collapse, and interaction of such system at elevated temperatures. More research contributions enable engineers to successfully analyse the structural performance and seismic behaviour of SPSW system in multi-hazard scenarios after being exposed to fire condition.

Figure 1. Steel plate shear wall system [25]

This research study aims to assess the post-fire seismic behaviour of SPSW system. It was assumed that the investigated models supported by a moment-resisting steel frame and SPSW systems are exposed to fire condition and subsequently an earthquake occurs which tests the models' resiliency after experiencing seismic excitation following the fire incident .

The reason for choosing a dual system of moment-resisting steel frame and SPSW for investigation was its widespread use in the regions with high levels of seismicity. More importantly, the post-fire earthquake scenario was chosen for investigation because this system has not been fully studied under such scenario as stated in the literature review section . In this study, post-fire seismic coefficients of steel structures with a dual moment-resisting steel frame and special low-yielding SPSW system were calculated and investigated using finite element simulation and performing a nonlinear static analysis.

2. Methodology

2.1. Assessment Procedure

The procedure adopted in this research was to assess the seismic performance of models after being exposed to fire or to investigate the post-fire seismic performance of models by comparing seismic coefficients of models . The flowchart shown in Figure 2 summarizes the adopted procedure . At first, for validating the finite element simulation procedure of the models an assembly of SPSW was modelled and compared with the experimental results. After achieving acceptable consistency between the simulated model and the experimental test, a set of models consisting of 3 structures of 3, 6, and 9-storey with dual systems of moment-resisting steel frame and low-yielding SPSW were designed 3-dimensionally according to specific standard codes. Next , 2D frames from the proposed models were selected. The assessment was carried out using 2D models for simplicity and saving computational resources. Since finite element modelling was already validated in the previous step, the simulation of the 2D finite element frame models was carried out consistently. At this important step, simulated 2D frames were divided in two groups, a group consisting of the models with the mechanical properties of steel at ambient temperature which were considered the initial cases, and in the second group the post-fire mechanical properties of steel at elevated temperatures during various fire scenarios were collected from a set of accredited experimental tests and were assigned to the models which were considered to be the post-fire cases. So, these two investigating groups each consisted of three structures, the initial cases with pre-fire mechanical properties of steel, and the post-fire cases with post-fire mechanical properties of steel. Next , both groups of initial cases and post-fire cases were assessed using push-over analysis, and the results of this analysis which was the push-over curve led to calculating response modification factors. Finally, response modification factors obtained from both cases were compared and investigated to draw practical conclusions regarding the post-fire seismic performance of the proposed models.

It should be clarified that the objective of this study was to investigate the post-fire seismic performance of the models using the response modification factor as an indicator of the structural seismic capacity. Also, it is essential to note that the effect of elevated temperatures on steel as a material results in two major changes, first the reduction in values of mechanical properties, and second the creation of residual stresses and large deformations. Amongst these two major changes, only the reduction in values of mechanical properties can affect the response modification factor. In addition, as a fundamental principle, it is understood that fire exposure leads to large deformations and residual stresses. However, the ultimate strength of steel remains the same even though it experiences lower values of plastic strain. Therefore, since the present study only seeks to assess the response modification factor of the models and not the structural behaviour, there was no need to consider large deformations of the models under fire scenarios because in the process of calculating this factor the consideration of large deformations is not effective.

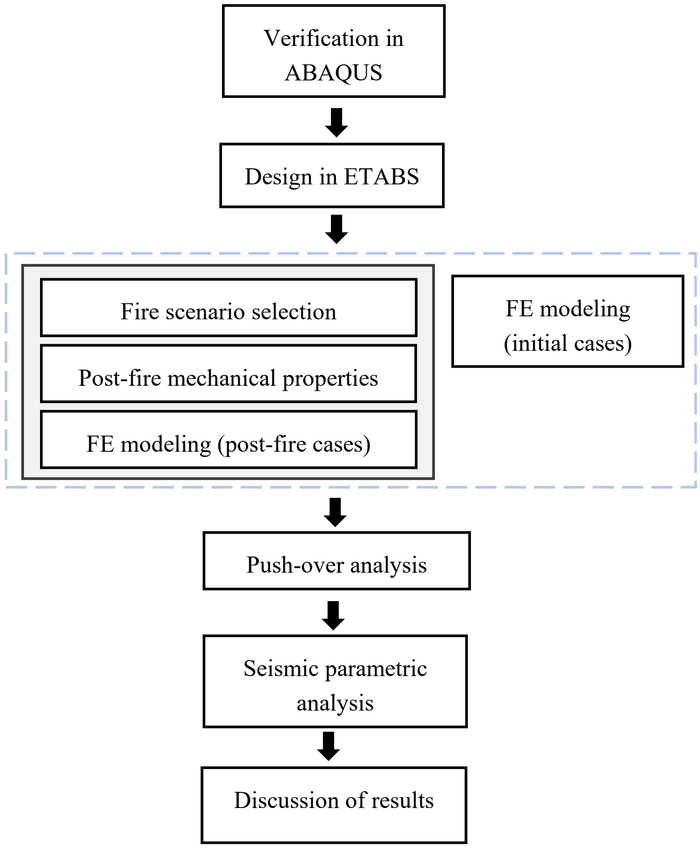

Figure 2. Flowchart of the assessment procedure

2.2. Seismic Coefficients

Estimation of structural seismic forces using linear-elastic analysis needs modification according to prescriptions made by standard codes. These forces are modified using a strength reduction factor or response modification factor to account for the inelastic behaviour of the structures. This factor is a function of different factors such as ductility, overstrength, etc. Lower values of this factor lead to the structural design of buildings with larger and noneconomical sections (overdesign), and higher values tend to accept higher levels of structural damage in designed structures. Overall, the application of the response modification factor allows designers to consider the inelastic response of structures in the design process without performing any inelastic analysis. The response modification factor satisfies the demanded strength consideration of structures by adding the ductility capacity.

For calculating the response modification factor of structures, the Uang method [26] was chosen since it has easier to comprehend compared to other methods. In this method, by equalizing the capacity curve into a bilinear graph, all the required characteristics of the structure's behavior will be extracted. For bilinearization of the curve, it has to be noted that the area under the bilinear graph must be equal to the area under the push-over graph, and by putting the slope of the first section of the bilinear graph to the push-over graph and coinciding the final point of these two graphs, the bilinear graph is produced. Figure 3 indicates a graph that presents the overall structural behavior and shows how a bilinear graph is plotted.

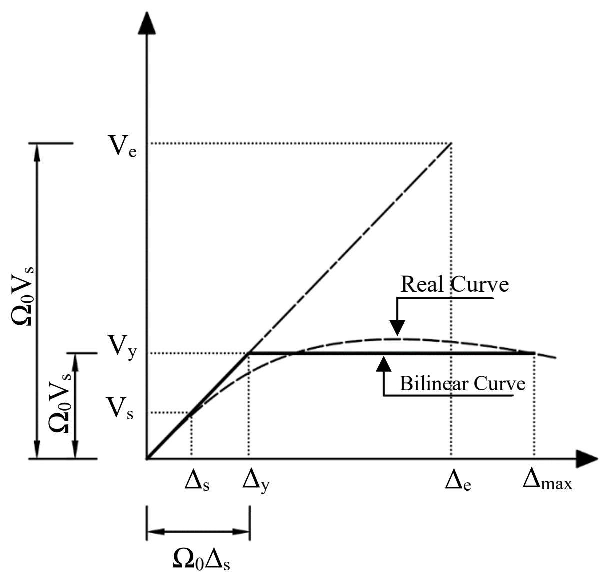

Figure 3. Overall structural behavior graph [26]

According to the Uang method, the required seismic coefficients for calculating the response modification factor can be calculated as following [26]:

$$R = R_\mu \Omega \qquad (1)$$

$$R_\mu = \frac{V_e}{V_y} \qquad (2)$$

$$\Omega = \frac{V_y}{V_s} \qquad (3)$$

In which, R_μ is the ductility reduction factor and Ω is the overstrength factor. R_μ is calculated by dividing ultimate applied forces on structure (V_e) over equivalent force to yielding limit of structure at the time of damage mechanism formation (V_y). Ω is calculated by dividing the equivalent force to the yielding limit of structure at the time of damage mechanism formation (V_y) over the equivalent force to the first plastic-hinge formation in structure (V_s) [26].

3. Finite Element Modelling

3.1. Model Validation

To validate any finite element (FE) model, it needs to be compared with experimental tests. In this study, a numerical assembly was modelled using finite element modelling (FEM) package, ABAQUS [27], which it was used for calibrating the result and checking the accuracy and compatibility of the proposed models. An experimental test carried out on an assembly of steel plate shear wall [28] was selected as the benchmark sample for validating the FE model. As can be seen in Figure 4(a), the test assembly consists of a steel panel as the shear wall, two steel columns, and two steel beams restraining the whole assembly as a rigid set.

In the process of FE modelling of the experimental test by ABABQUS [27], the nonlinear static analysis was performed, and as for the loading step it was applied laterally at the top left corner of the assembly as an incremental displacement boundary condition until reaching the target of 70 mm which was considered to be the allowable drift of the assembly. FE model was respectively restrained with hinge supports and lateral supports on the bottom and top sides of the layout. For modelling the assembly parts, S4R shell elements (4 nodes with reduced integration) were selected, and by carrying out a mesh sensitivity analysis, element size of 20 mm proved to be compatible with test results. In addition, a buckling analysis was performed to gather the imperfection values to enable the steel plate to correctly deform . Figure 4(b) depicts the meshed assembly set with 20 mm size elements.

Figure 4(c) illustrates the deformed shape of the modelled test assembly. Also, Figure 4(d) shows the achieved push-over curve which proves that the results of the FE model with 20 mm size elements are in acceptable agreement with experimental results. By validating the FE model based on the deformed shape and the push-over curve, it can be concluded that the FE simulation process carried out in this study was accurate.

(a)

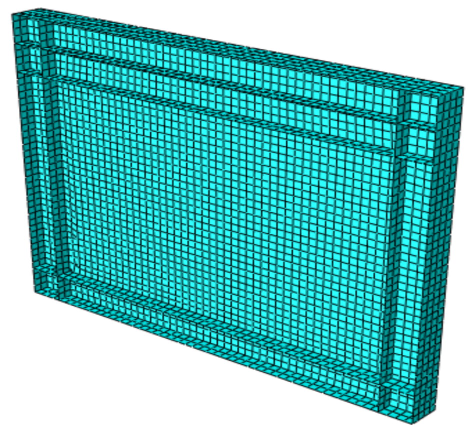

(b)

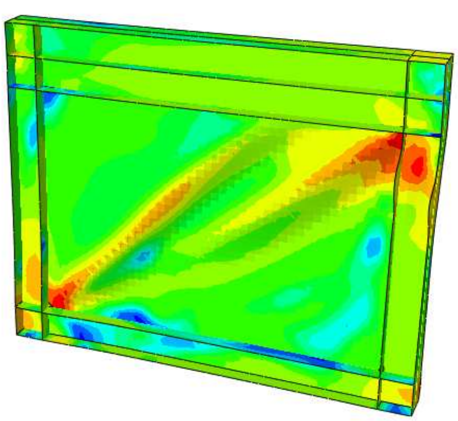

(c)

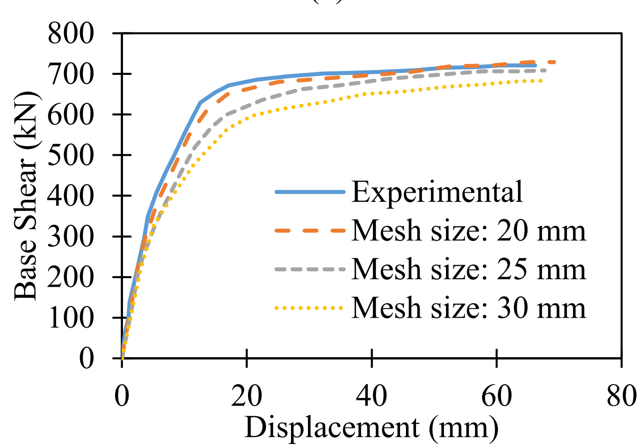

(d)

Figure 4. (a) Deformed shape of the experimental test assembly [28] (b) Meshed assembly set (c) Deformed shape of the FE model (d) Push-over curve comparing the result of FE model with experimental test (mesh sensitivity analysis)

3.2. Investigated Models

To investigate the role of fire incidents on seismic coefficients of structures under different fire scenarios, 3 structures of 3, 6, and 9-storey were chosen to be designed. Since these proposed structural models have dual systems of moment-resisting steel frame and steel plate shear walls, the shear wall systems were designed manually according to AISC-341/16 [29], then other structural members were designed using CSI ETABS [30] according to the considerations of ASCE-7/16 [31] and AISC-360/16 [32].

Proposed structural models were considered residential buildings with dual systems of moment-resisting steel frame and SPSW , located in the city of Los Angeles (United States) with seismic parameters of S_s (spectral acceleration at short periods) equal to 2.433 and S_1 (spectral acceleration at a period of 1 sec) equal to 0.853. In addition, design parameters according to ASCE-7/16 [31] were considered to be response modification factor (R) equal to 8, overstrength factor (Ω_0) equal to 2.5, and displacement amplification factor (C_d) equal to 6.5 with site soil class C ($366 < V_s < 762$ m/s). The steel used for structural members except for shear walls was considered to have a yielding strength equal to 2400 kg/cm^2 and an elastic modulus of 2.1E+6 kg/cm^2, but for shear walls, a low-yielding steel with yielding strength of 1000 kg/cm^2 and elastic modulus of 2.0E+6 kg/cm^2 was considered , and Poisson ratio of 0.4 was assumed for both steel types. The geometry of structures was considered regular both in plan and height with a span length of 5 m and a storey height of 3.2 m. Also, the thickness of the steel plate shear walls for 3-storey model was assumed 2 mm for the 1st storey, 1.5 mm for the 2nd storey, and 1 mm for the 3rd storey. For the 6-storey model, the thicknesses were assumed 2.5 mm for the 1st and 2nd stories, 2 mm for the 3rd and 4th

stories, and 1.5 mm for the 5th and 6th stories. Also, the shear walls plates in the 9-storey model had a thickness of 3 mm for the 1st to 3rd stories, 2.5 mm for the 4th to 6th stories, and 2 mm for the 7th to 9th stories. Figures 5(a), (c), and 5(e) illustrate the 3D view of the designed structures.

3.3. Numerical Simulation

After the structural design of the models, since they were all regular in plan and height, a frame from each structure with a SPSW system was chosen to be modelled 2-dimensionally by ABAQUS [27].

After the fabrication of assembly parts, mechanical property values of steel for both shear wall and other structural members were applied as stated earlier as an isotropic material . All the connections were tied as rigid elements to other parts, and the bottom support of the models was tied to the ground as rigid elements too. Modelled structures were meshed using S4R shell elements (4 nodes with reduced integration). Gravity load on the beams was applied as linear distributed load, and lateral load applied on the modelled structures was considered as a reverse triangular loading case. Subsequently, structures were pushed from one side in a horizontal direction until reaching the target displacement using the specified loading condition. ASCE-7/16 [31] recommends the following formula for calculating target displacement based on the type of modelled structures:

$$\Delta_a = 0 \cdot 02h \qquad (4)$$

In which, Δ_a is the maximum roof drift and h is the height of the structure. By entering the height of each structure, the target displacement of 3, 6, and 9-storey structures equalled to 19.2 cm, 38.4 cm, and 57.6 cm. Since peripheral frames in the modelled structures are lateral load-bearing frames and interior frames of the structures only carry gravity loads, under seismic excitation , because of the mass of interior frames , peripheral frames are subjected to seismic acceleration which eventually forms the lateral loading conditions and lateral loading forces must be resisted by the peripheral frames equally because of the nonlinear static analysis attempt [33]. For this purpose, a column known as the P-Δ column was attached to the modelled structures to carry the resulted forces of interior frames' weight which were the subjected gravity loads on interior frames, and were applied as a point load on P-Δ/Leaning column [34]. The connection of this column to the main structures must be considered as hinge supports both on the lateral side and ground. The element chosen for modelling this column was wire with an elastic modulus of 2.0E+20 kg/cm^2 and a Poisson ratio of 0.4 [35-38]. Figure 5(g) illustrates the position of the P-Δ/Leaning column and the application of the triangular loading case [35-38].

Modelled structures are shown in Figures 5(b, d, and f). These models were analysed using the nonlinear static method (push-over) and subjected to triangular loading conditions until reaching calculated target displacement as initial cases before applying fire scenarios, and each model was titled by its number of stories, SPSW (steel plate shear wall), and the name "initial", for instance, the primary 3-storey model is titled 3SPSW-initial.

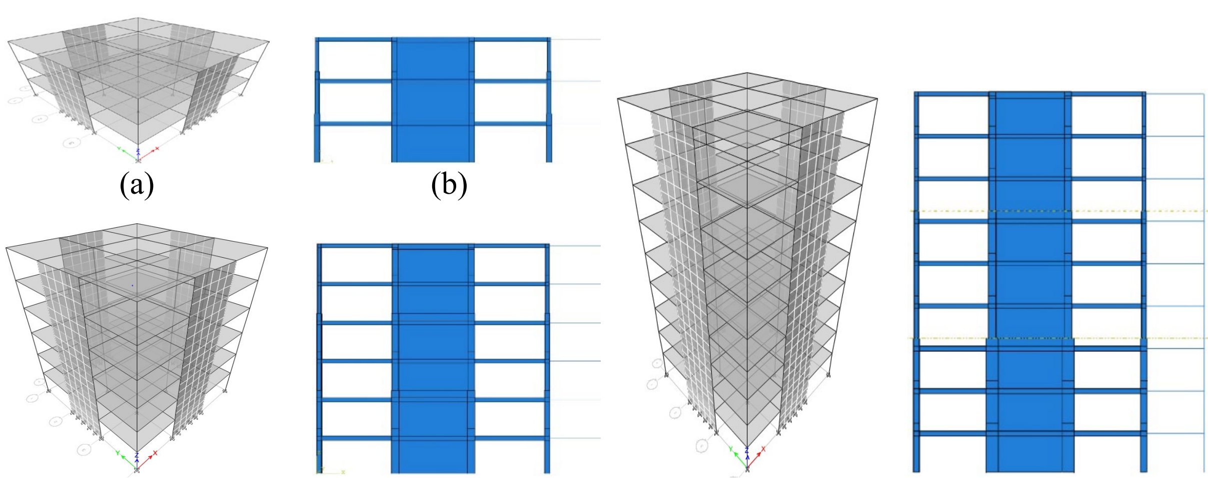

(a) (b)

(c) (d) (e) (f)

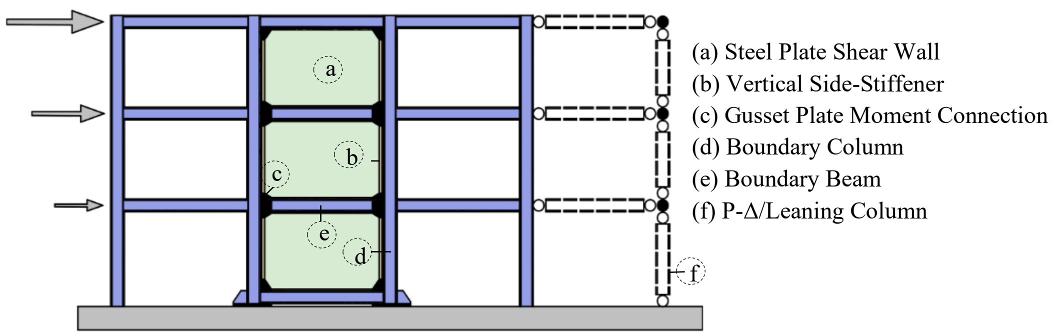

(g)

Figure 5. (a, c, and e) 3D view of the 3, 6, and 9-storey models (b, d, and f); FE modelled structures as 3SPSW-initial, 6SPSW-initial, and 9SPSW-initial (g) Illustration of P-Δ/Leaning column and triangular loading on a 3-storey model

3.4. Fire Scenarios

Steel is a widely used material in the construction industry and is prone to the risk of fire incidents [1]. At the time of fire exposure, steel members are exposed to elevated temperatures which will eventually may trigger the collapse, partial damage, or reduced structural capacity of the fire-damaged structure. If the structure does not collapse, for determining the extent of imposed damage and deciding about the replacement or rehabilitation of the damaged members , the residual capacity (strength) of the structure must be carefully investigated.

In this study, the effect of the heating was considered by applying post-fire residual mechanical properties (as given in reference [39]) of steel to the frame models. The post-fire mechanical properties of the adopted steel are based on experimental tests subject to a process of heating to 1000°C and 800°C then cooling by water and air. In the experimental test, applied heating process was accomplished by a temperature-controlled electric furnace for adjusting the heating rate and in this heating process uniform temperature distribution on the specimens were ensured and exceeding actual temperature from the target temperature was avoided. Subsequently, the specimens were removed from the furnace and cooled down to ambient temperature. Both air and water cooling methods were considered. Specimens cooled by air were exposed to air and allowed to be cooled down at their rates to simulate the situation in which a fire puts out naturally.

Specimens cooled by water were cooled down by water spray using a water jet to simulate the scenario in which fire is extinguished by sprinklers . . In addition, this study proposes a set of predictive equations for calculating the mechanical properties of structural steel at elevated temperatures which can be generalised to use for various steel types [39]. Following equations were used for calculating the required mechanical properties of steel types used for the models both frame and the shear wall system [39]:

Elastic Modulus, under air cooling condition,

$$20°\mathrm{C} \leq \mathrm{T} \leq 800°\mathrm{C} \rightarrow \frac{\mathrm{E_{PT}}}{\mathrm{E}} = 1 \qquad (5)$$

$$800°\mathrm{C} < \mathrm{T} \leq 1000°\mathrm{C} \rightarrow \frac{\mathrm{E_{PT}}}{\mathrm{E}} = 2 \cdot 148 - 2 \cdot 15 \times 10^{-3}\mathrm{T} + 9 \cdot 02 \times 10^{-7}\mathrm{T}^2 \qquad (6)$$

under water cooling condition,

$$20°\mathrm{C} \leq \mathrm{T} \leq 800°\mathrm{C} \rightarrow \frac{\mathrm{E_{PT}}}{\mathrm{E}} = 1 \qquad (7)$$

$$800°\mathrm{C} < \mathrm{T} \leq 1000°\mathrm{C} \rightarrow \frac{\mathrm{E_{PT}}}{\mathrm{E}} = 2 \cdot 891 - 4 \cdot 27 \times 10^{-3}\mathrm{T} + 2 \cdot 23 \times 10^{-6}\mathrm{T}^2 \qquad (8)$$

In which, E_{PT} is the elastic modulus after cooling down from elevated temperatures, E is the elastic modulus at room temperature and T is the temperature in °C.

Yield Stress, under air cooling condition,

$$20°\mathrm{C} \leq \mathrm{T} \leq 700°\mathrm{C} \rightarrow \frac{\mathrm{f_{yPT}}}{\mathrm{f_y}} = 1 \qquad (9)$$

$$700°\mathrm{C} < \mathrm{T} \leq 1000°\mathrm{C} \rightarrow \frac{\mathrm{f_{yPT}}}{\mathrm{f_y}} = 1 \cdot 6 - 8 \cdot 88 \times 10^{-4}\mathrm{T} \qquad (10)$$

under water cooling condition,

$$20°\mathrm{C} \leq \mathrm{T} \leq 600°\mathrm{C} \rightarrow \frac{\mathrm{f_{yPT}}}{\mathrm{f_y}} = 1 \cdot 007 + 2 \cdot 17 \times 10^{-5}\mathrm{T} \qquad (11)$$

$$600°\mathrm{C} < \mathrm{T} \leq 1000°\mathrm{C} \rightarrow \frac{\mathrm{f_{yPT}}}{\mathrm{f_y}} = 1 \cdot 313 - 4 \cdot 75 \times 10^{-4}\mathrm{T} \qquad (12)$$

In which, f_{yPT} is the yield stress after cooling down from elevated temperatures, f_y is the yield stress at room temperature and T is the temperature in °C.

Ultimate Stress, under air cooling condition,

$$20°\mathrm{C} \leq \mathrm{T} \leq 1000°\mathrm{C} \rightarrow \frac{f_{uPT}}{f_u} = 0 \cdot 999 + 1 \cdot 59 \times 10^{-4}\mathrm{T} - 2 \cdot 89 \times 10^{-7}\mathrm{T}^2 \qquad (13)$$

under water cooling condition,

$$20°\mathrm{C} \leq \mathrm{T} \leq 1000°\mathrm{C} \rightarrow \frac{f_{uPT}}{f_u} = 0 \cdot 990 + 2 \cdot 57 \times 10^{-4}\mathrm{T} - 5 \cdot 91 \times 10^{-7}\mathrm{T}^2 + 3 \cdot 16 \times 10^{-10}\mathrm{T}^3 \qquad (14)$$

In which, f_{uPT} is the ultimate stress after cooling down from elevated temperatures, f_u is the ultimate stress at room temperature and T is the temperature in °C.

Based on the above equations, the mechanical properties of the used steel types are calculated as shown in Table 1, and by using these values plastic behavior of the steel was predicted to be implemented in the FE simulations.

Table 1. Post-fire mechanical properties of steel

Steel type and Initial properties	Properties	Temperature (°c) 800		1000	
		Cooling method: Air	Water	Air	Water
MRF elements: $f_y = 2400$ kg/cm^2, $f_u = 3700$ kg/cm^2, E = 2.1E+6 kg/cm^2, $\varepsilon_y = 0.0011428$	E	2.1E+6	2.1E+6	1.89E+6	1787100
	f_y	2135.04	2239.2	1708.8	2011.2
	f_u	3482.588	3622.8624	3215.3	3596.4
	ε_y	0.0010166	0.00106628	0.0009041	0.00112539
	ε_u	0.19	0.155	0.185	0.105
	ε_p	0.1889834	0.15393372	0.1840959	0.10387461
SPSWs: $f_y = 1000$ kg/cm^2, $f_u = 2600$ kg/cm^2, E = 2E+6 kg/cm^2, $\varepsilon_y = 0.0005$	E	2E+6	2E+6	1.8E+6	1702000
	f_y	889.6	933	712	838
	f_u	2447.224	2545.7952	2259.4	2527.02
	ε_y	0.0004448	0.0004665	0.0003955	0.00049236
	ε_u	0.19	0.155	0.185	0.105
	ε_p	0.1895552	0.1545335	0.1846045	0.10450764

In total, 64 scenarios were analysed considering various temperatures, cooling methods, and the location of fire exposure which are summarized in Table 2. Knowing that prediction of where fire initiates and to which direction it spreads in a building depend on various factors [23], these assumptions were designed based on major fire incidents in the world [24].

FE models noted in this table are introduced in the following : the first number denotes the number of stories, SPSW indicates it's a steel plate shear wall, the second number denotes the number of the storey(s) exposed to the fire scenario, the number 800 or 1000 shows considered fire temperature and air (a) or water (w) shows the cooling process. For instance, 9SPSW-7/8/9-1000-a case is the 9-storey structure subjected to 1000°C fire temperature at stories 7, 8, and 9, which are then cooled by air.

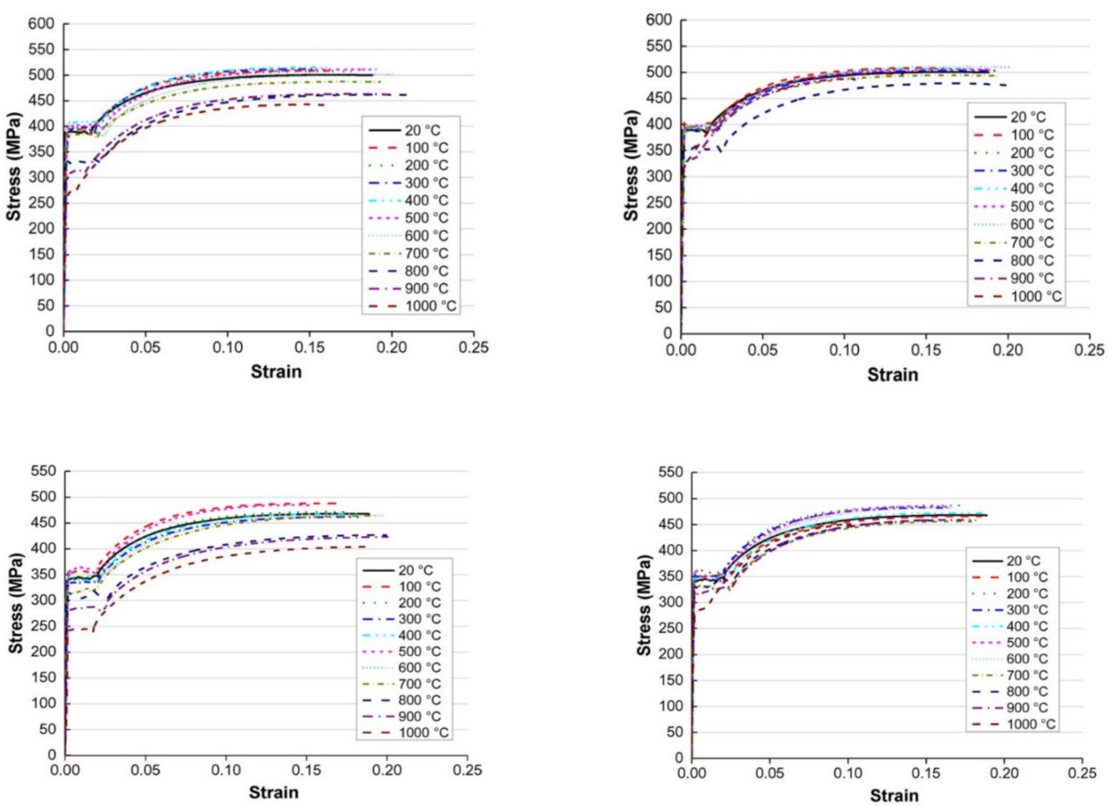

Table 2. Assumed fire scenarios

St...	Temperature (°C)	
	800	**1000**

	Stories exposed to fire	Cooling method			
		Air	Water	Air	Water
3	1st	3SPSW-1-800-a	3SPSW-1-800-w	3SPSW-1-1000-a	3SPSW-1-1000-w
	2nd	3SPSW-2-800-a	3SPSW-2-800-w	3SPSW-2-1000-a	3SPSW-2-1000-w
	3rd	3SPSW-3-800-a	3SPSW-3-800-w	3SPSW-3-1000-a	3SPSW-3-1000-w
	1st + 2nd	3SPSW-1/2-800-a	3SPSW-1/2-800-w	3SPSW-1/2-1000-a	3SPSW-1/2-1000-w
6	1st + 2nd	6SPSW-1/2-800-a	6SPSW-1/2-800-w	6SPSW-1/2-1000-a	6SPSW-1/2-1000-w
	2nd + 3rd	6SPSW-2/3-800-a	6SPSW-2/3-800-w	6SPSW-2/3-1000-a	6SPSW-2/3-1000-w
	3rd + 4th	6SPSW-3/4-800-a	6SPSW-3/4-800-w	6SPSW-3/4-1000-a	6SPSW-3/4-1000-w
	4th + 5th	6SPSW-4/5-800-a	6SPSW-4/5-800-w	6SPSW-4/5-1000-a	6SPSW-4/5-1000-w
	5th + 6th	6SPSW-5/6-800-a	6SPSW-5/6-800-w	6SPSW-5/6-1000-a	6SPSW-5/6-1000-w
	1st to 4th	6SPSW-1/2/3/4-800-a	6SPSW-1/2/3/4-800-w	6SPSW-1/2/3/4-1000-a	6SPSW-1/2/3/4-1000-w
9	1st to 3rd	9SPSW-1/2/3-800-a	9SPSW-1/2/3-800-w	9SPSW-1/2/3-1000-a	9SPSW-1/2/3-1000-w
	3rd + 4th	9SPSW-3/4-800-a	9SPSW-3/4-800-w	9SPSW-3/4-1000-a	9SPSW-3/4-1000-w
	4th to 6th	9SPSW-4/5/6-800-a	9SPSW-4/5/6-800-w	9SPSW-4/5/6-1000-a	9SPSW-4/5/5-1000-w
	6th + 7th	9SPSW-6/7-800-a	9SPSW-6/7-800-w	9SPSW-6/7-1000-a	9SPSW-6/7-1000-w
	7th to 9th	9SPSW-7/8/9-800-a	9SPSW-7/8/9-800-w	9SPSW-7/8/9-1000-a	9SPSW-7/8/9-1000-w
	1st to 6th	9SPSW-1/2/3/4/5/6-800-a	9SPSW-1/2/3/4/5/6-800-w	9SPSW-1/2/3/4/5/6-1000-a	9SPSW-1/2/3/4/5/6-1000-w

4. Performance Assessment

4.1. Structural Assessment

FE model assemblies were pushed to target displacements by nonlinear static analysis in two separate procedures, one before exposure to fire as initial cases and another after the heating-cooling process according to the prescribed fire scenarios as post-fire cases . The first stage of investigation was the structural assessment of the deformed elements of the FE models in terms of stress distribution based on the Von Mises stress contours criterion. Figures 6 to 8, respectively illustrate stress contours of pre-fire (initial case) and post-fire deformed FE models of 3, 6, and 9-storey structures. Figures compare the pre-fire and post-fire deformed shapes of each structure after push-over analysis separately in two sections of steel plate shear wall system and moment-resisting steel frame system. Due to the high number of fire scenarios, only deformed shapes of FE models with the most severe fire scenarios were chosen to be compared with initial pre-fire cases, and the most severe ones are selected by the number of stories that are exposed to fire and cooled by water such as 3SPSW-1/2-1000-W, 6SPSW-1/2/3/4-1000-W, 9SPSW-1/2/3/4/5/6-1000-W. The overall structural assessment of both types of models (pre-fire and post-fire) revealed that stress concentration is specifically located around the connection zones, bottom beams, columns, and steel panels of shear walls. Stress concentration decreases upward from down to top floors which shows the reverse relation of lateral forces to base shear forces in a laterally pushed case. It is quite clear that the lateral load-bearing system within the steel frame (SPSW) in all of the cases is experiencing more intense stress distributions because it is responsible for carrying the major portion of lateral loading cases. Also, by comparing pre-fire and post-fire cases, it can be understood that the yielding stress capacity of moment-resisting steel frames as shown in terms of stress contours has remained constant which can be explained due to the lower reduced values of mechanical properties of steel after heating to 1000°C and being water cooled instantly. But in case of SPSW systems, it was observed that yielding stress capacity in post-fire models is decreased compared to initial cases, denoting that deformed shapes of post-fire models indicate lower values of yielding stress which proves to be an obvious reduction in their post-fire structural strength. Referring to Table 1, reduced values of mechanical properties of moment-resisting steel frames' steel after exposure to 1000°c fire and being cooled by water on average is less than 12% of the initial values while in the case of SPSWs' steel the same heating-cooling process reduces its properties to less than 20% on average. So, this considerable difference between reduced values clearly explains different structural performances , but since both of the structural systems are acting continuously tied to each other as one integrated load-bearing system, the overall reduction in the structural performance of post-fire cases compared to initial cases is seen as the average response of both systems .

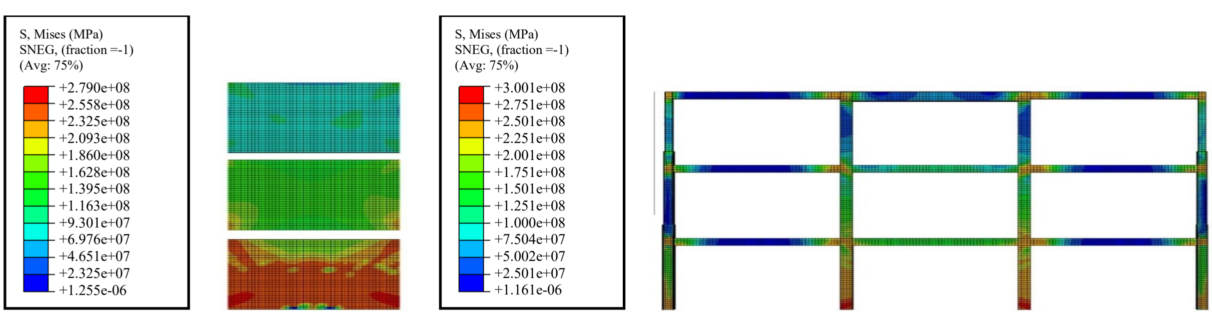

(a)

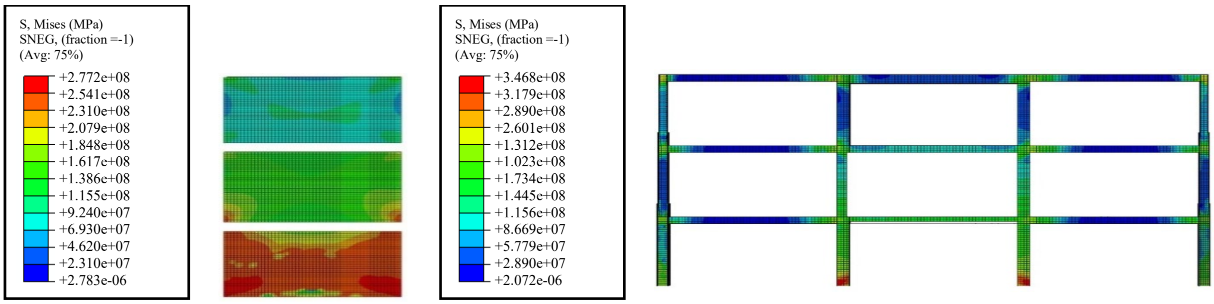

(b)

Figure 6. Stress distribution contours of (a) Initial case (b) 3SPSW-1/2-1000-W

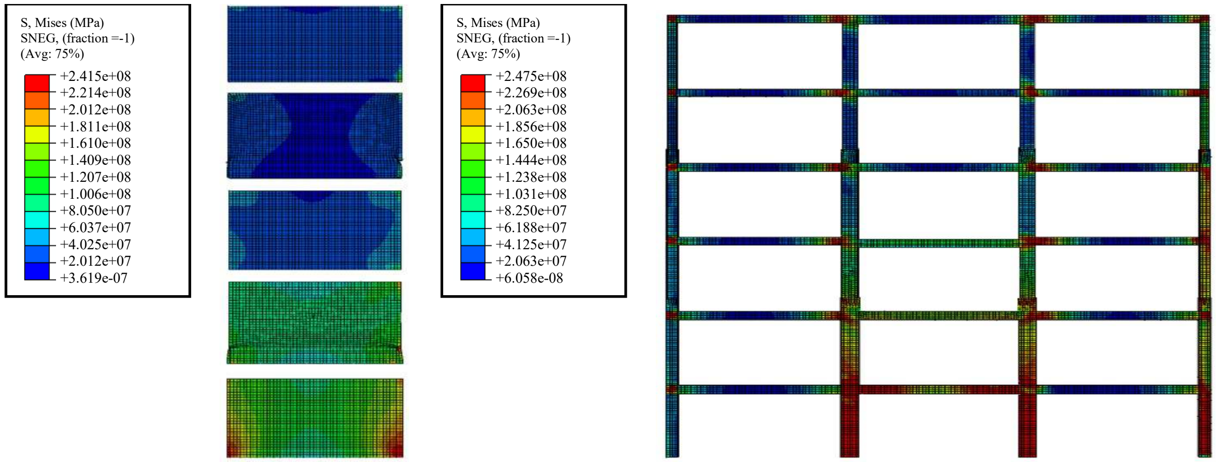

(a)

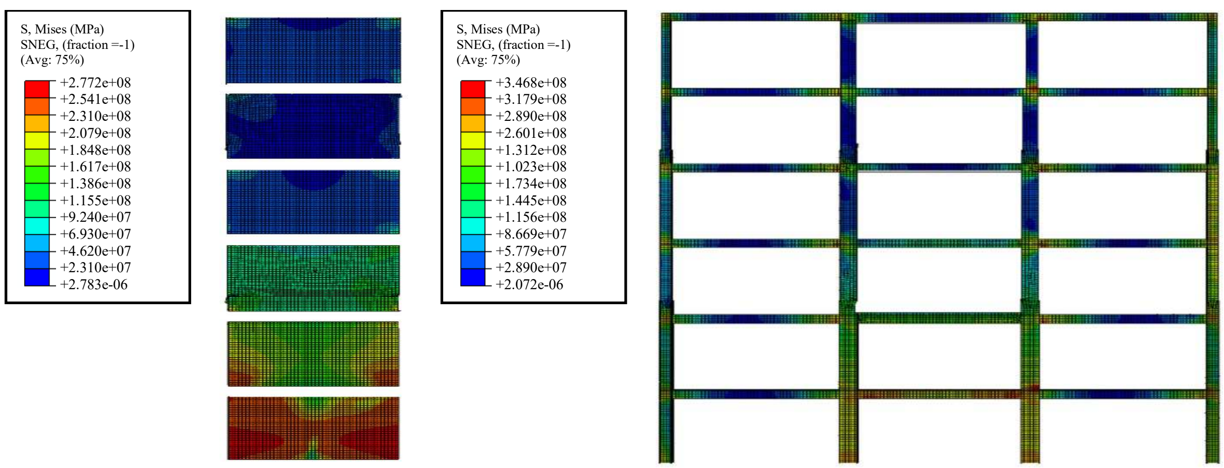

(b)

Figure 7. Stress distribution contours of (a) Initial case (b) 6SPSW-1/2/3/4-1000-W

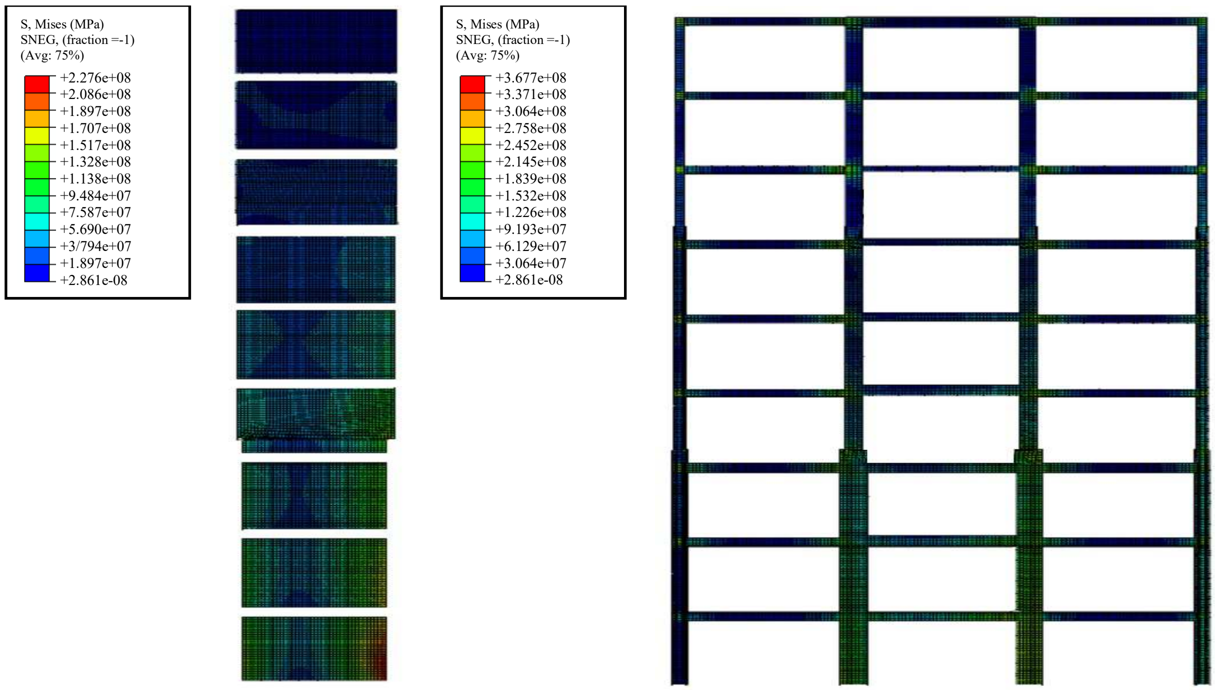

(a)

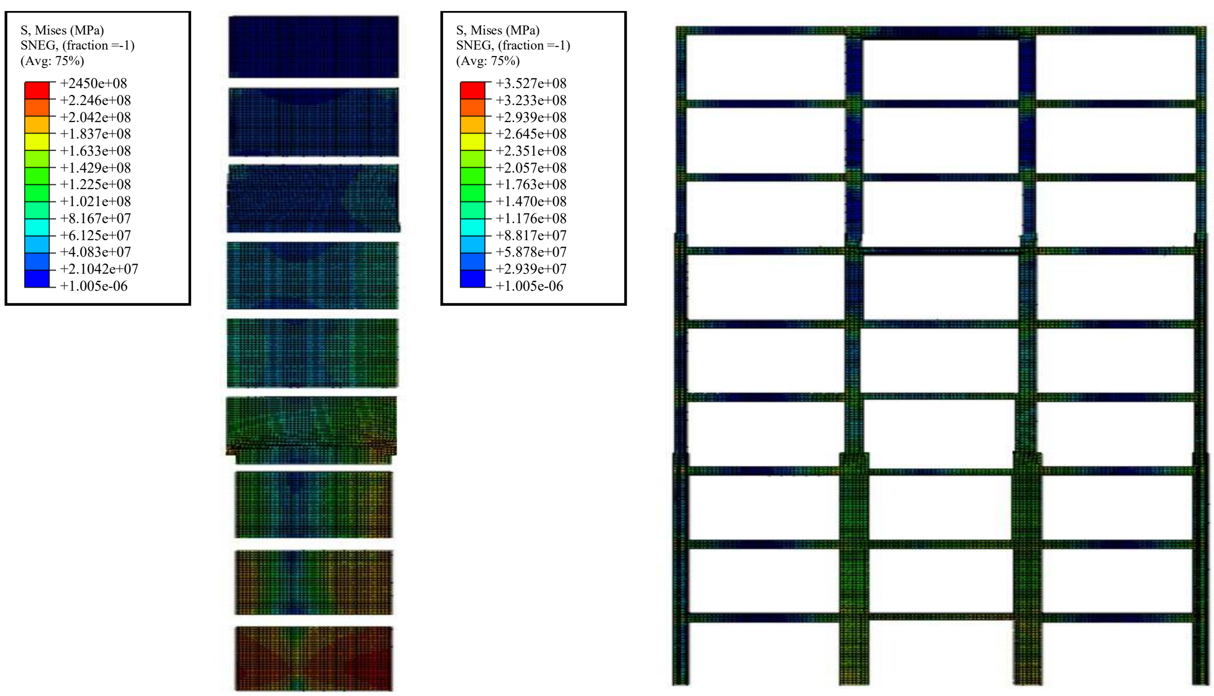

(b)

Figure 8. Stress distribution contours of (a) Initial case (b) 9SPSW-1/2/3/4/5/6-1000-w

4.2. Post-Fire Seismic Performance

Push-over analysis results of the nonlinear static analysis are extracted in terms of base shear to displacement until reaching the calculated target displacement of each case. To compare the acquired results and analyse the levels of reduction in the base shear forces at target displacement between structures under various fire scenarios, Figure 9 illustrates column charts presenting maximum base shear forces of 3, 6, and 9-storey structures respectively at calculated target displacements of 19.2 cm, 38.4 cm, and 57.6 cm at all the considered fire scenarios separately.

It can be observed from all the column charts that base shear force has reduced in all the structures after applying fire scenarios compared with initial cases which shows the negative effect of fire. Values of base shear in fire scenarios that air cooling process has been employed, in most cases were decreased more than water cooling process which denotes the effect of the cooling process on preserving the residual capacity of the exposed building structures in real-time scenarios. Also, it can be understood that with increasing the intensity of the fire scenario in terms of the number of stories getting involved, the residual base shear capacity of burning structures was reduced considerably, for instance, in all three structures, the application of the most severe fire scenario has resulted in the reduction of base shear capacity by almost half the initial value. So, the type of cooling process and severity of fire scenarios can clearly act as counter factors against the post-fire seismic performance of structures, and notably water cooling seems to be a better option for putting out of fire because it seems that it reduces the heating temperature quicker than air cooling and eventually cuts the cooling process shorter than air cooling which will give the burning structure less time to undergo hazardous effects of fire exposure. This positive contribution of water cooling method is greatly dependent of the higher specific heat of water compared to air.

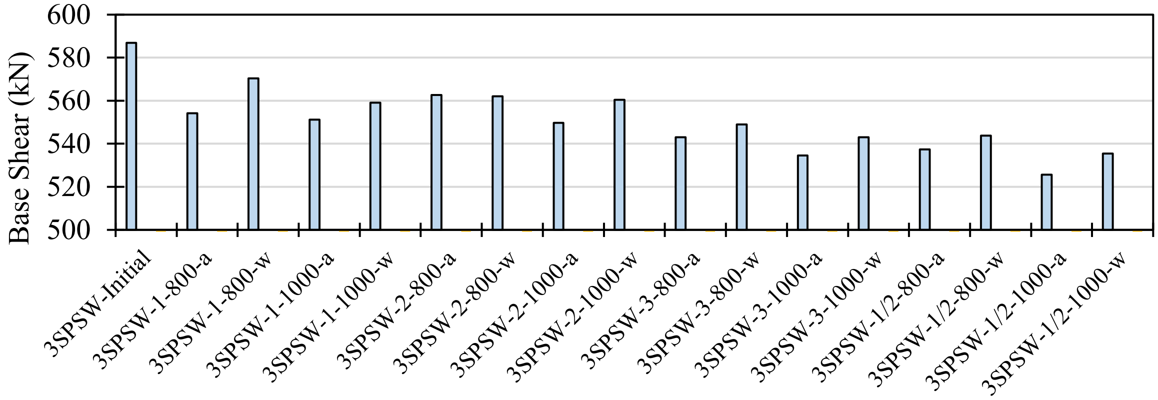

(a)

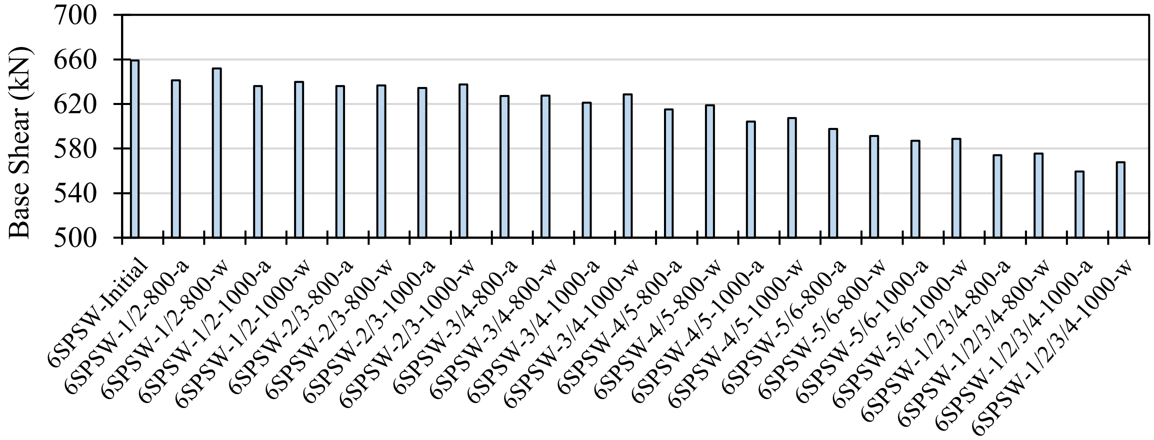

(b)

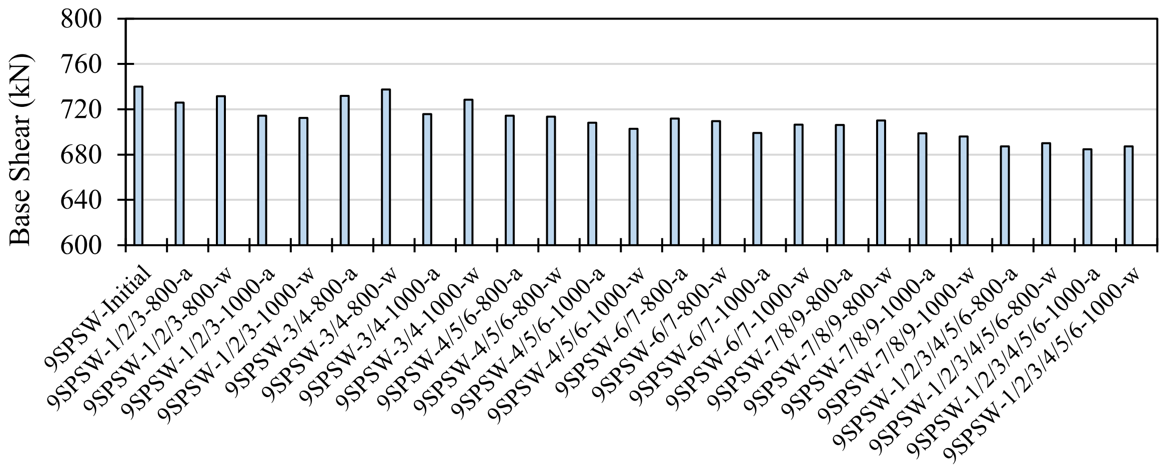

(c)

Figure 9. Comparison of maximum base shear at target displacement for; (a) 3-storey, (b) 6-storey, and (c) 9-storey structures

4.3 Calculation of Seismic Coefficients

By using the results of push-over curves illustrated in the previous section plus interpolation and mathematical computations, parameters required for calculating seismic coefficients of the investigated structures were calculated . Using linear interpolation for calculating unknown parameters by having the first and last points of the push-over curve and the slope of the first section of the curve the area of the push-over curve was computed as a parametric equation (2^{nd} order equation which x is the point where push-over curve breaks) and by putting it equal to the known area of the graph, x was computed and by having the slope value, y was acquired too. So, known values of x and y helped to compute the parameters of V_s, V_y, and V_e that led to the calculation of seismic coefficients R_μ and Ω which eventually value of R or response modification factor was achieved.

In addition to the calculation of the response modification factor and other parameters, the area under the push-over curve was computed using the trapezoid method . Respectively, the calculated area of the curves or dissipated energy (A), overstrength factor (Ω), ductility reduction factor (R_μ), and response modification factor (R) for each structure under different scenarios is illustrated by the column charts shown in Figures 10 to 12.

It can be observed that the 3SPSW-initial case has the maximum amount of A and 3SPSW-1/2-1000-a case with 2 stories exposed to the fire of 1000°c and cooled by air has the minimum value of A which compared to the initial case has experienced 11.73% reduction . Maximum and minimum values of R_μ relate to 3SPSW-1/2-1000-a and 3SPSW-1/2-800-a cases with respectively 4.4% increase and 8.8% decrease compared to the initial case. In addition, it can be understood from the chart that cases of 3SPSW-initial and 3SPSW-1/2-1000-a have the maximum and minimum values of Ω with an 18.44% difference. Also, it can be observed by the column chart that 3SPSW-initial and 3SPSW-1/2-1000-a cases have the maximum and minimum values of R with a difference of about 14.91%. Except 3SPSW-1-1000-a case, it can be perceived that cooling by water conduces lower levels of reduction in the values of the response modification factor of models in various fire scenarios.

In the case of 6-storey models, the 6SPSW-initial case has the maximum amount of A and the 6SPSW-1/2/3/4-1000-a case with 4 stories exposed to the fire of 1000°c and cooled by air has the minimum value of A which compared to the initial case has experienced 13.32% reduction . Maximum and minimum values of R_{μ} relate to 6SPSW-4/5-1000-a and 6SPSW-1/2/3/4-1000-a cases with respectively 1.78% increase and 6.25% decrease compared to the initial case. In addition, it can be understood from the chart that cases of 6SPSW-initial and 6SPSW-1/2/3/4-1000-a have the maximum and minimum values of Ω with a 10.14% difference. Also, it can be observed by the column chart that 6SPSW-initial and 6SPSW-1/2/3/4-1000-a cases have the maximum and minimum values of R with a difference of about 15.85%. Except 6SPSW-4/5-1000-a case, it can be perceived that air cooling tends to reduce the response modification factor of models more than water cooling in various fire scenarios.

Results of the 9-storey cases indicate that the 9SPSW-initial case has the maximum amount of A and 9SPSW-1/2/3/4/5/6-1000-a case with 6 stories exposed to the fire of 1000°c and cooled by air has the minimum value of A which compared to the initial case has experienced 7.13% reduction . Maximum and minimum values of R_{μ} relate to 9SPSW-7/8/9-800-a and 9SPSW-1/2/3/4/5/6-1000-a cases with respectively 2.18% increase and 4% decrease compared to the initial case. In addition, it can be understood from the chart that cases of 9SPSW-initial and 9SPSW-7/8/9-800-a have the maximum and minimum values of Ω with an 8.19% difference. Also, it can be observed by the column chart that 9SPSW-initial and 9SPSW-1/2/3/4/5/6-1000-a cases have the maximum and minimum values of R with a difference of about 9.03%. It can be concluded that cooling by water reduces models' response modification factors less than air cooling in different fire scenarios.

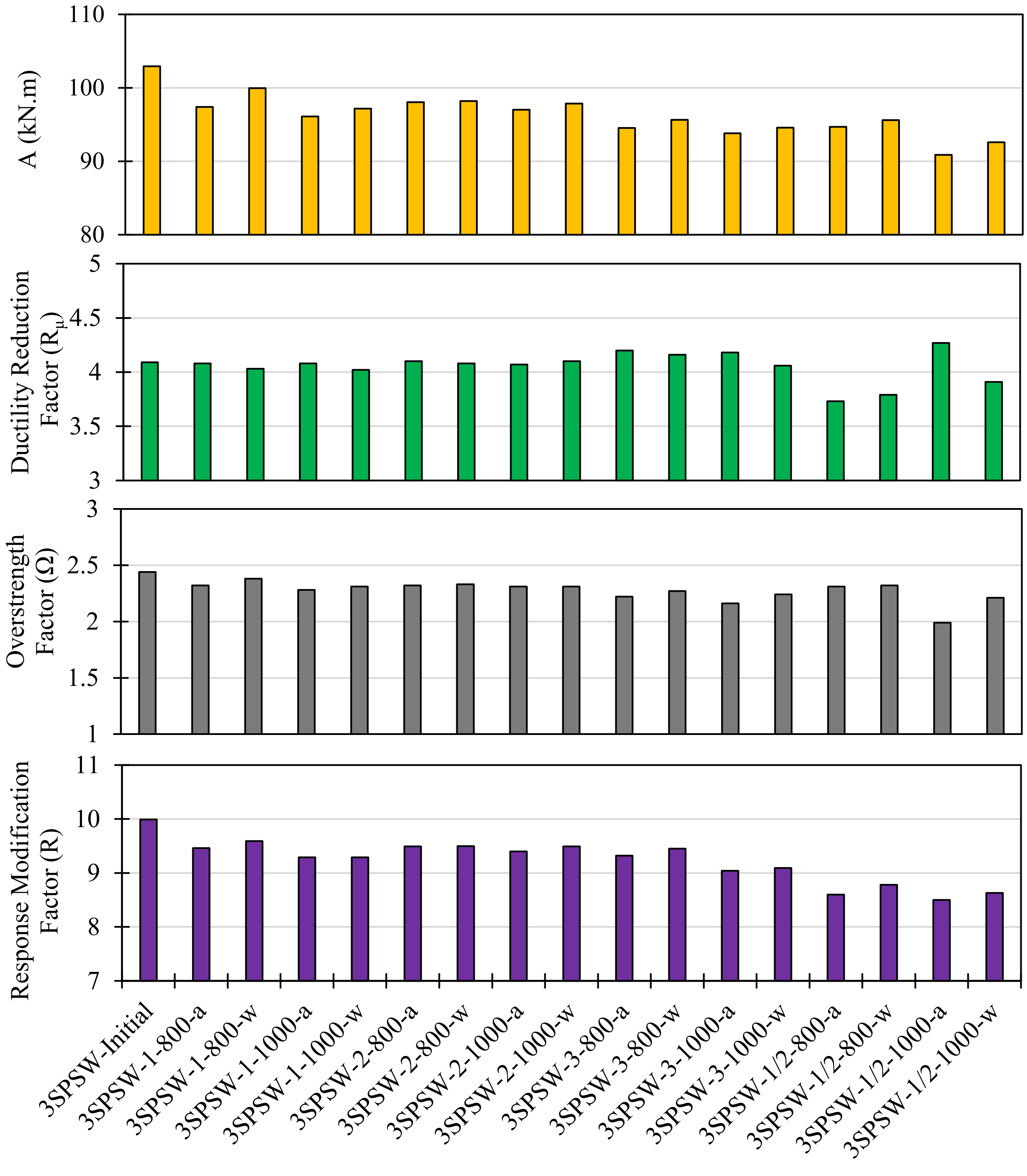

Figure 10. Comparison of seismic coefficients for all the 3-storey cases

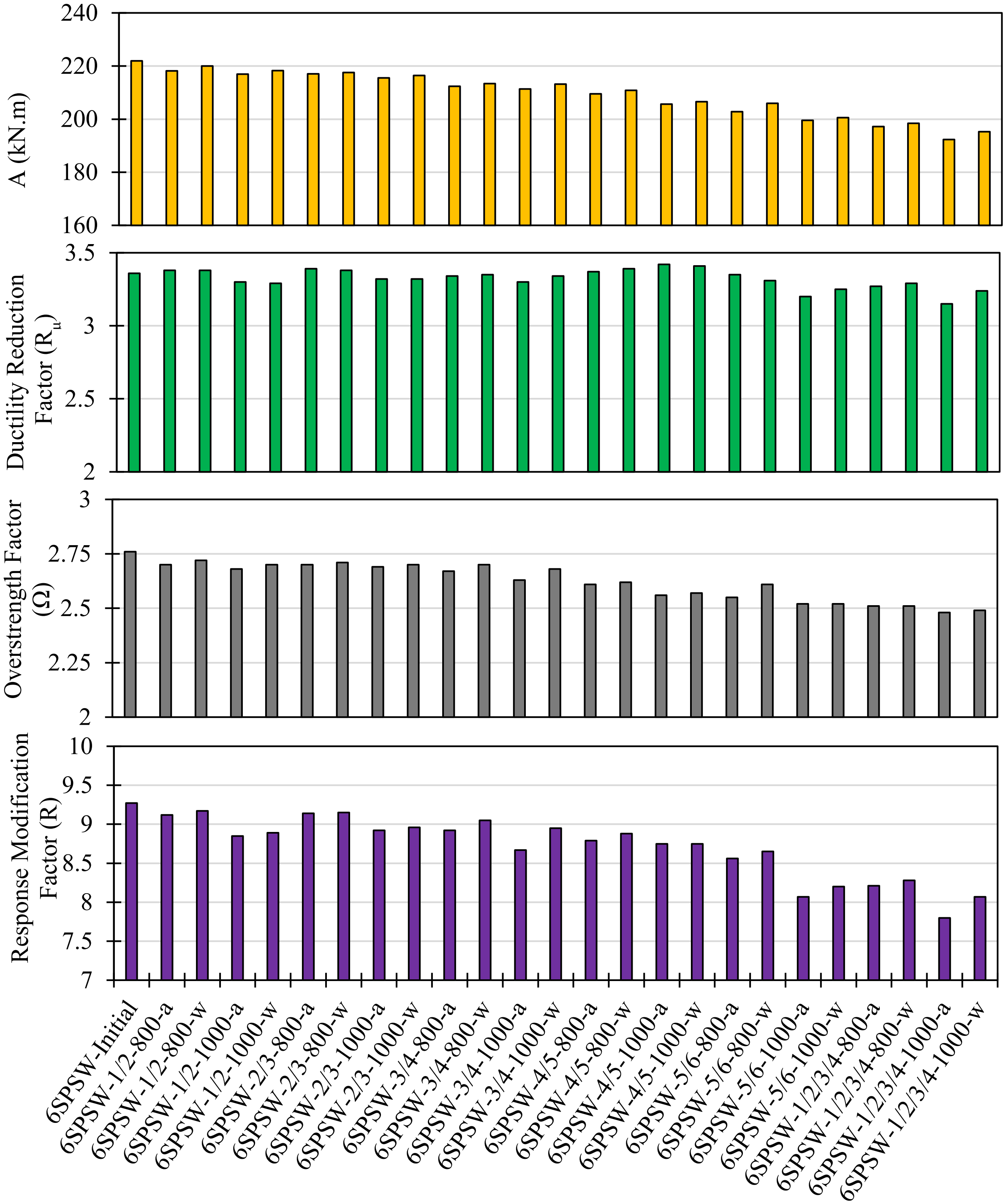

Figure 11. Comparison of seismic coefficients for all the 6-storey cases

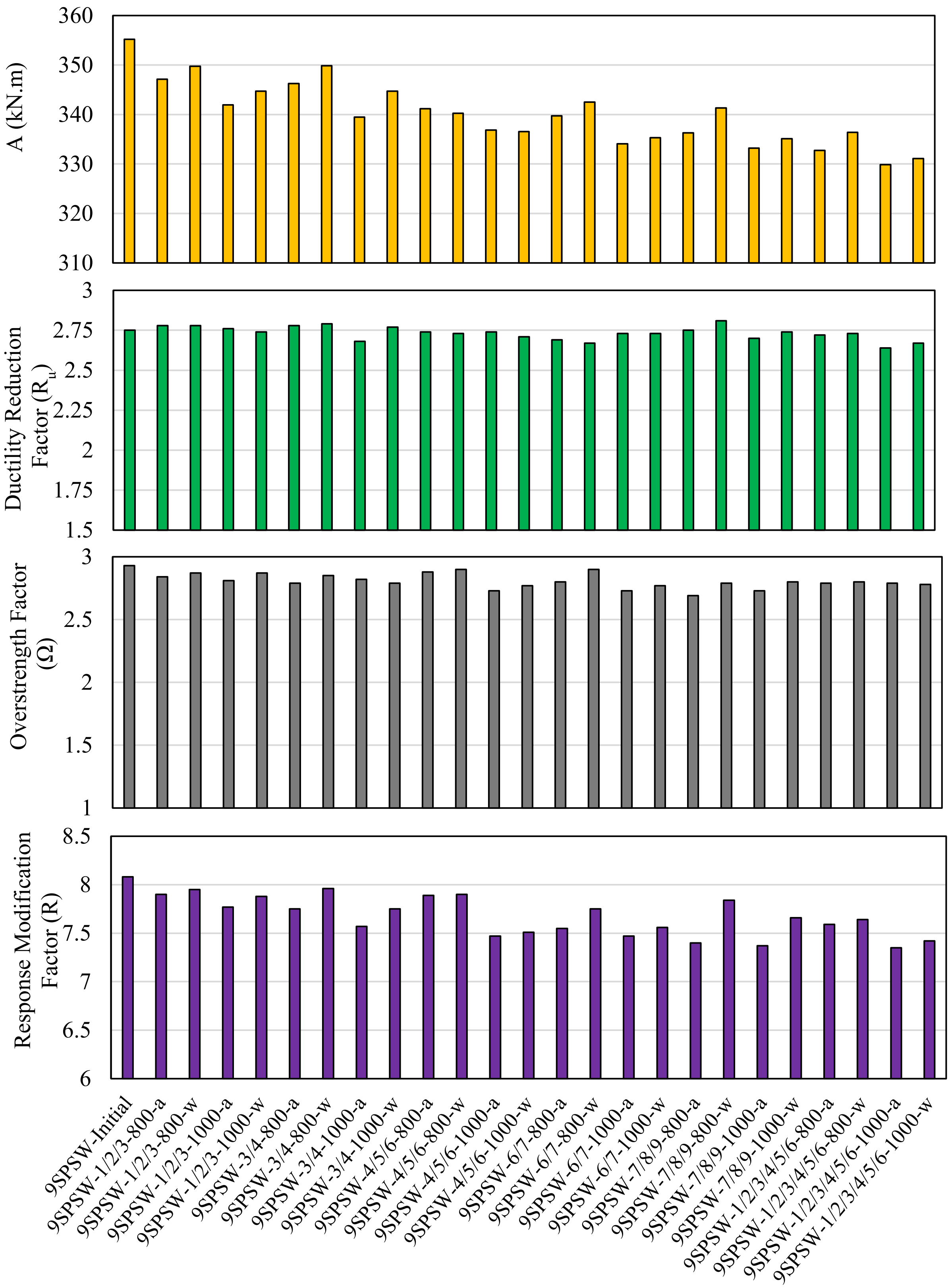

Figure 12. Comparison of seismic coefficients for all the 9-storey cases

5. Summary and Conclusions

This paper presents a study investigating the post-fire seismic performance of moment-resisting steel frames with low-yielding steel plate shear walls. Three structures of 3, 6, and 9 stories were considered. Nonlinear static push-over analysis was conducted on the FE models to determine their target displacements before and after fire exposure. To consider the effect of fire, the post-fire residual mechanical properties of steel were applied to the FE models. Also, it has to be noted that in this study it was sought to assess the response modification factor of the models, and there was no need to consider large deformations of the models under fire scenarios because in the process of calculating this factor the consideration of large deformations is not effective. Various temperatures, cooling methods, and fire exposure locations were assumed . The results of analyses were extracted as push-over graphs (Base Shear-Displacement). Using the Uang method, the seismic coefficients of each structure under the considered scenarios were determined and compared. The conclusions of this work are summarized below. It should be noted that these conclusions are drawn from the investigated models. More research is still required to draw more generalized conclusions.

- Values of A (dissipated energy) in 3, 6, and 9-storey initial cases of 3SPSW-initial, 6SPSW-initial, and 9SPSW-initial are respectively calculated as 107 kN.m, 222 kN.m, and 355.2 kN.m which clearly show that increase in height results in an increase of energy dissipation.

- Comparison of values of A (dissipated energy) shows that the cases with most stories exposed to the fire of 1000°c and cooled by air have the least values of A. The cases of 3SPSW-1/2-1000-a, 6SPSW-1/2/3/4-1000-a, and 9SPSW-1/2/3/4/5/6-1000-a respectively have rounded A values of 91 kN.m, 192.4 kN.m, and 330 kN.m which are considered as the minimum values of A amongst various fire scenarios for 3, 6 and 9-storey FE models.

- In cases of 3SPSW-initial, 6SPSW-initial, and 9SPSW-initial, the values of R_μ (ductility reduction factor) are respectively 4.09, 3.36, and 2.75 which indicate the reverse relationship of height with this factor.

- Comparison of values of R_μ shows that cases with most stories exposed to fire, fire temperatures of 1000°c and cooled by air have the least values of R_μ; cases of 3SPSW-1/2-1000-a, 6SPSW-1/2/3/4-1000-a, and 9SPSW-1/2/3/4/5/6-1000-a respectively have rounded R_μ values of 3.73, 3.15, and 2.64 which are considered as the minimum values of R_μ amongst various fire scenarios for 3, 6, and 9-storey FE models.

- Calculated values of Ω (overstrength factor) in 3, 6, and 9-storey initial cases of 3SPSW-initial, 6SPSW-initial, and 9SPSW-initial are approximately 2.44, 2.76, and 2.93 which indicate that by increasing the height, the overstrength factor increases too.

- In 3 and 6-storey FE models cases with most stories under fire condition, fire temperatures of 1000°c and being air cooled; cases of 3SPSW-1/2-1000-a, and 6SPSW-1/2/3/4-1000-a respectively have the values of Ω equal to 1.99 and 2.48 registered as the least values compared to other cases, and between 9-storey cases with 3 stories under fire condition, fire temperatures of 800°c and being air cooled, 9SPSW-7/8/9-800-a has the minimum value of Ω equal to 2.69.

- In cases of 3SPSW-initial, 6SPSW-initial, and 9SPSW-initial, values of R (response modification factor) are respectively 9.99, 9.27, and 8.08 which indicates the reverse relationship of height with response modification factor.

- Comparison of the calculated values of R (response modification factor) indicates that cases with most stories exposed to fire, fire temperatures of 1000°c and being cooled by air have the least values of R; cases of 3SPSW-1/2-1000-a, 6SPSW-1/2/3/4-1000-a, and 9SPSW-1/2/3/4/5/6-1000-a respectively have the approximate values of R equal to 8.5, 7.8, and 7.35 which are considered as the minimum values of R amongst various fire scenarios for 3, 6, and 9-storey FE models. In a percentage-wise comparison, the post-fire response modification factors of 3, 6, and 9-storey FE models are respectively reduced by 14.9%, 15.9%, and 9.0%.
- Based on the recommendation of ASCE-7/16, the value of R for the considered type of structural system is 8. On the other hand, the minimum calculated post-fire value of R amongst all the FE models considered in this study was 7.35 (which belongs to a 9-storey structure). So, it can be concluded that the code-specified value of R is rather conservative even in the post-fire calculations.

Finally, based on the calculated values of seismic coefficients, it can be stated that heating-cooling processes with water cooling tend to reduce the values of seismic coefficients less than air cooling which can be considered a significant issue in firefighting, rehabilitation, and post-fire seismic assessment of structures under various fire scenarios in real-time incidents.

6. Recommendations and Limitations

It is recommended for future works that instead of using post-fire mechanical properties of steel a heat transfer analysis carries out before the push-over analysis in the FEM simulation process. Also, it is suggested to experimentally test the post-fire seismic performance of this system in a scenario in which the assembly gets heated and after cooling down by various methods it undergoes a push-over test by applying lateral force. Furthermore, fire scenarios, heating temperatures, and types of cooling methods can be studied variably to investigate their effect on the residual seismic performance of such systems too.

References

[1] Safari, P. and Broujerdian, V., 2020, December. Strategies to increase the survivability of steel connections in fire. In *Structures* (Vol. 28, pp. 2335-2354). Elsevier. https://doi.org/10.1016/j.istruc.2020.10.033

[2] Mohammadi Dehcheshmeh, E., Rashed, P., Broujerdian, V., Shakouri, A. and Aslani, F., 2023, Predicting Seismic Collapse Safety of Post-Fire Steel Moment Frames. *Buildings*, 13, 1091. https://doi.org/10.3390/ buildings13041091

[3] Ni, S., Yan, X., Hoehler, M. and Gernay, T., 2021, December. Finite element analysis of the lateral capacity of cold-formed steel shear walls after fire exposure. Proceedings of the 12th Asia-Oceania Symposium on Fire Science and Technology, Brisbane, AU. https://doi.org/10.14264/0825e72

[4] Zhang, B., Yu, J., Chen, W., Wang, H. and Xu, J., 2020. Stress states and shear failure mechanisms of girders with corrugated steel webs. *Thin-Walled Structures*, *157*, p.106858. https://doi.org/10.1016/j.tws.2020.106858

[5] Glassman, J.D., Boyce, V. and Garlock, M.E.M., 2019. Effectiveness of stiffeners on steel plate shear buckling at ambient and elevated temperatures. *Engineering Structures*, *181*, pp.491-502. https://doi.org/10.1016/j.engstruct.2018.12.012

[6] Samiee, P., Niari, S.E. and Ghandi, E., 2021, February. Fire performance of cold-formed steel shear wall with different steel grade and thicknesses. In *Structures* (Vol. 29, pp. 751-770). Elsevier. https://doi.org/10.1016/j.istruc.2020.11.073

[7] Andres, B., Hoehler, M.S. and Bundy, M.F., 2020. Fire resistance of cold-formed steel framed shear walls under various fire scenarios. *Fire and materials*, *44*(3), pp.352-364. https://doi.org/10.1002/fam.2744

[8] Hoehler, M.S., Andres, B. and Bundy, M.F., 2020. Lateral resistance reduction to cold-formed steel-framed shear walls under various fire scenarios. *Journal of Structural Engineering*, *146*(5), p.04020066. https://doi.org/10.1061/(ASCE)ST.1943-541X.0002610

[9] Ni, S., Yan, X., Hoehler, M.S. and Gernay, T., 2022. Numerical modeling of the post-fire performance of strap-braced cold-formed steel shear walls. *Thin-Walled Structures*, *171*, p.108733. https://doi.org/10.1016/j.tws.2021.108733

[10] Hutchinson, T.C., Wang, X., Hegemier, G., Kamath, P. and Meacham, B., 2021. Earthquake and Postearthquake Fire Testing of a Midrise Cold-Formed Steel-Framed Building. I:

Building Response and Physical Damage. *Journal of Structural Engineering*, *147*(9), p.04021125. https://doi.org/10.1061/(ASCE)ST.1943-541X.0003097

[11] Wang, X. and Hutchinson, T.C., 2021. Earthquake and Postearthquake Fire Testing of a Midrise Cold-Formed Steel-Framed Building. II: Shear Wall Behavior and Design Implications. *Journal of Structural Engineering*, *147*(9), p.04021126. https://doi.org/10.1061/(ASCE)ST.1943-541X.0003098

[12] Jamshidi, M., NaserAbadi, H.D. and Oliaei, M., 2020. Performance of steel-plate shear wall at high temperature. *Journal of Structural Fire Engineering*. https://doi.org/10.1108/JSFE-02-2020-0005

[13] Hoehler, M.S. and Smith, C.M., 2016. Influence of fire on the lateral load capacity of steel-sheathed cold-formed steel shear walls-report of test. US Department of Commerce, National Institute of Standards and Technology. https://doi.org/10.6028/nist.ir.8160

[14] Hoehler, M.S., Smith, C.M., Hutchinson, T.C., Wang, X., Meacham, B.J. and Kamath, P., 2017. Behavior of steel-sheathed shear walls subjected to seismic and fire loads. *Fire safety journal*, *91*, pp.524-531. https://doi.org/10.1016/j.firesaf.2017.03.021

[15] Yu, Y., Lan, L., Ding, F. and Wang, L., 2019. Mechanical properties of hot-rolled and cold-formed steels after exposure to elevated temperature: A review. *Construction and Building Materials*, *213*, pp.360-376. https://doi.org/10.1016/j.conbuildmat.2019.04.062

[16] Zhou, X., Xue, X., Shi, Y. and Xu, J., 2021. Post-fire mechanical properties of Q620 high-strength steel with different cooling methods. Journal of Constructional Steel Research, 180, p.106608. https://doi.org/10.1016/j.jcsr.2021.106608

[17] Shi, G., Wang, S., Chen, X. and Rong, C., 2021. Post-fire mechanical properties of base metal and welds of Q235 steel. Journal of Constructional Steel Research, 183, p.106767. https://doi.org/10.1016/j.jcsr.2021.106767

[18] Hua, J., Wang, F., Xue, X., Sun, Y. and Gao, Y., 2023. Post-fire ultra-low cycle fatigue properties of high-strength steel via different cooling methods. Thin-Walled Structures, 183, p.110406. https://doi.org/10.1016/j.tws.2022.110406

[19] Xia, Y., Yan, X., Gernay, T. and Blum, H.B., 2022. Elevated temperature and post-fire stress-strain modeling of advanced high-strength cold-formed steel alloys. *Journal of Constructional Steel Research*, *190*, p.107116. https://doi.org/10.1016/j.jcsr.2021.107116

[20] Guo, Y., Fang, C. and Zheng, Y., 2021. Post-fire hysteretic and low-cycle fatigue behaviors of Q345 carbon steel. *Journal of Constructional Steel Research*, *187*, p.106991. https://doi.org/10.1016/j.jcsr.2021.106991

[21] Yu, B., Chen, Z., Wang, P. and Song, X., 2023. A comparative study on the mechanical behavior of S355J2 steel repair-welded joints. *Journal of Constructional Steel Research*, *205*, p.107878. https://doi.org/10.1016/j.jcsr.2023.107878

[22] Pańcikiewicz, K., Maślak, M., Pazdanowski, M., Stankiewicz, M. and Zajdel, P., 2023. Changes in the microstructure of selected structural alloy steel grades identified after their simulated exposure to fire temperature. *Case Studies in Construction Materials*, *18*, p.e01923. https://doi.org/10.1016/j.cscm.2023.e01923

[23] Behnam, B. and Ronagh, H.R., 2014. Behavior of moment-resisting tall steel structures exposed to a vertically traveling post-earthquake fire. *The Structural Design of Tall and Special Buildings*, *23*(14), pp.1083-1096. https://doi.org/10.1002/tal.1109

[24] Fu, F., 2021. *Fire Safety Design for Tall Buildings*. CRC Press.

[25] Seilie, I.F. and Hooper, J.D., 2005. Steel plate shear walls: practical design and construction. *Modern steel construction*, *45*(4), pp.29-33.

[26] Uang, C.M., 1991. Establishing R (or Rw) and Cd factors for building seismic provisions. *Journal of structural Engineering*, *117*(1), pp.19-28. https://doi.org/10.1061/(ASCE)0733-9445(1991)117:1(19)

[27] ABAQUS: Abaqus/CAE user's manual. Providence, RI, USA: Dassault Systems; 2014.

[28] Alavi, E. and Nateghi, F., 2013. Experimental study on diagonally stiffened steel plate shear walls with central perforation. *Journal of Constructional Steel Research*, *89*, pp.9-20. https://doi.org/10.1016/j.jcsr.2013.06.005

[29] AISC Committee, 2016. Seismic Provision for Structural Steel Buildings (ANSI/AISC 341-16).

[30] CSI, C., 2016. Analysis reference manual for SAP2000, ETABS, and SAFE. *Computers and Structures, Berkeley, California, USA*.

[31] American Society of Civil Engineers, 2016, Minimum design loads and associated criteria for buildings and other structures (ASCE 7-16).

[32] Ansi, B., 2016. AISC 360-16, specification for structural steel buildings. *Chicago AISC*.

[33] Sabouniaghdam, M., Mohammadi Dehcheshmeh, E., Safari, P. and Broujerdian, V., 2022. Probabilistic collapse assessment of steel frame structures considering the effects of soil-structure interaction and height. *Scientia Iranica*, *29*(6), pp.2979-2994. https://doi.org/10.24200/SCI.2022.58707.5860

[34] Broujerdian, V., Mohammadi Dehcheshmeh, E. and Safari, P., 2023. Seismic performance assessment of intermediate moment-resisting steel frames designed based on misidentified site soil classes. *Scientia Iranica*. https://doi.org/10.24200/SCI.2023.60650.6915

[35] Mohammadi Dehcheshmeh, E. and Broujerdian, V., 2022. Determination of optimal behavior of self-centering multiple-rocking walls subjected to far-field and near-field ground motions. Journal of Building Engineering, 45, p.103509. https://doi.org/10.1016/j.jobe.2021.103509

[36] Majumerd, M.J.E., Dehcheshmeh, E.M., Broujerdian, V. and Moradi, S., 2022. Self-centering rocking dual-core braced frames with buckling-restrained fuses. Journal of Constructional Steel Research, 194, p.107322. https://doi.org/10.1016/j.jcsr.2022.107322

[37] Broujerdian, V. and Mohammadi Dehcheshmeh, E., 2022. Locating the rocking section in self-centering bi-rocking walls to achieve the best seismic performance. Bulletin of Earthquake Engineering, 20(5), pp.2441-2468. https://doi.org/10.1007/s10518-022-01325-y.

[38] Mohammadi Dehcheshmeh, E. and Broujerdian, V., 2022. Probabilistic Evaluation of Self-Centering Birocking Walls Subjected to Far-Field and Near-Field Ground Motions. Journal of Structural Engineering, 148(9), p.04022134. https://doi.org/10.1061/(ASCE)ST.1943-541X.0003435

[39] Lu, J., Liu, H., Chen, Z. and Liao, X., 2016. Experimental investigation into the post-fire mechanical properties of hot-rolled and cold-formed steels. *Journal of constructional steel research*, *121*, pp.291-310. https://doi.org/10.1016/j.jcsr.2016.03.005